

Multinuclear NMR and Kinetic Analysis of DNA Interstrand Cross-Link Formation

Hui Ding,[†] Ananya Majumdar,^{*,‡} Joel R. Tolman,[†] and Marc M. Greenberg^{*,†}

Department of Chemistry and Biomolecular NMR Center, Johns Hopkins University,
3400 North Charles Street, Baltimore, Maryland 21218

Received October 4, 2008; E-mail: ananya@jhu.edu; mgreenberg@jhu.edu

Abstract: Recently, a phenylselenenyl-modified thymidine (**2**) was shown to produce DNA interstrand cross-links (ICLs) via two mechanisms. Photolysis of **2** generates 5-(2'-deoxyuridinyl)methyl radical (**1**), the reactive intermediate that results from formal hydrogen atom abstraction from the thymine methyl group. This reactive intermediate reacts with the opposing dA and is the first example of a DNA radical that produces ICLs. Kinetic competition studies support the proposal that the rate-limiting step in ICL formation from **1** involves rotation about the glycosidic bond and that the rate constant for this process is influenced by the flanking sequence. Cross-links also form with the opposing dA when **2** is treated with mild oxidants that result in the formation of an intermediate methide-like species (**4**). Kinetic experiments reveal that **4** reacts with azide, a model nucleophile, via an S_N2' pathway. Previous experiments suggested that the same product is produced via **1** or **4** but that the initially formed cross-link rearranges during the enzyme digestion and isolation procedures. In situ product analysis by NMR using synthetic, doubly labeled duplex DNA containing ¹³C-**2** and ¹⁵N₁-dA provides definitive evidence that the kinetic ICL products formed via the radical and oxidative pathways are the same and correspond to that arising from formal alkylation of N₁-dA. Furthermore, analysis of the thermodynamic product formed upon rearrangement indicates that the primary product isomerizes via an associative mechanism in DNA.

Introduction

DNA interstrand cross-links (ICLs) are responsible for the cytotoxicity of a number of antitumor agents.^{1,2} They are also produced via endogenous cellular lipid oxidation as well as by exogenous bis-electrophiles.^{3–5} The physiological effects of this DNA lesion family are frequently associated with their ability to block replication and transcription as well as the difficulty of their repair.^{1,6–8} Synthetically induced ICLs are also useful in a variety of biotechnology applications. These include control of gene expression in mammalian cells and sequence-specific recognition of DNA at single-nucleotide resolution.^{9,10} The importance of ICLs continues to spur creative approaches for

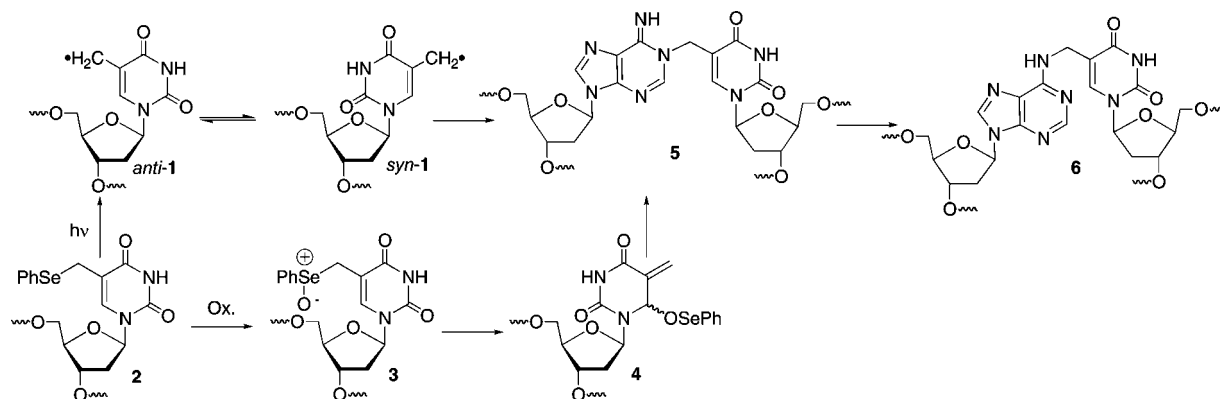
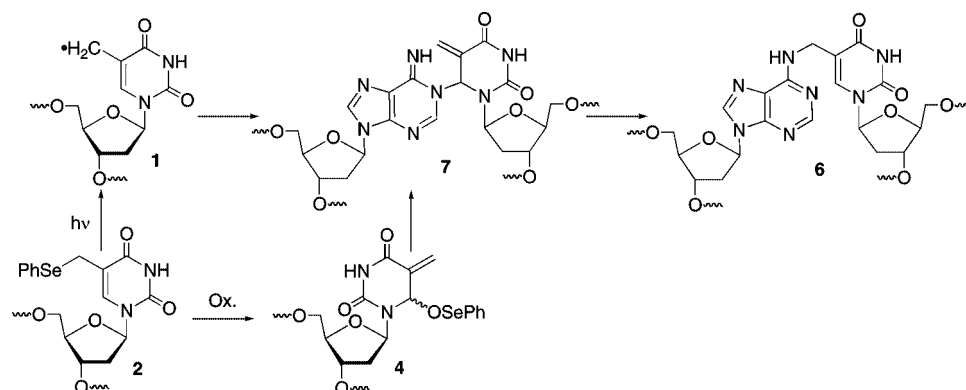
their formation.^{11–14} Recently, we discovered a process by which the DNA radical **1** generated via formal hydrogen atom abstraction from the thymine methyl group cross-links with the opposing dA in the duplex (Scheme 1).^{15,16} Although this transformation was originally detected using photolabile synthetic radical precursors (e.g., **2**), the ICL was subsequently identified in γ -irradiated DNA.¹⁷ This was the first characterization of an ICL produced in DNA by γ -radiolysis via a radical. ICLs are also produced from the phenyl selenide **2** under a variety of oxidative conditions following sigmatropic rearrangement of the selenoxide **3** (Scheme 1).^{15,18,19} This mild and rapid method for producing ICLs has been used to develop a method for detecting single-nucleotide polymorphisms.²⁰ In this application, covalent linkage between the biotinylated oligonucleotide probe and the target enhances selectivity by permitting

[†] Department of Chemistry.

[‡] Biomolecular NMR Center.

- (1) Noll, D. M.; Mason, T. M.; Miller, P. S. *Chem. Rev.* **2006**, *106*, 277–301.
- (2) Schärer, O. D. *ChemBioChem.* **2005**, *6*, 27–32.
- (3) Stone, M. P.; Cho, Y.-J.; Huang, H.; Kim, H.-Y.; Kozekov, I. D.; Kozekova, A.; Wang, H.; Minko, I. G.; Lloyd, R. S.; Harris, T. M.; Rizzo, C. J. *Acc. Chem. Res.* **2008**, *41*, 793–804.
- (4) Kozekov, I. D.; Nechev, L. V.; Moseley, M. S.; Harris, C. M.; Rizzo, C. J.; Stone, M. P.; Harris, T. M. *J. Am. Chem. Soc.* **2003**, *125*, 50–61.
- (5) Kim, H.-Y. H.; Voehler, M.; Harris, T. M.; Stone, M. P. *J. Am. Chem. Soc.* **2002**, *124*, 9324–9325.
- (6) Niedernhofer, L. J.; Lalai, A. S.; Hoeijmakers, J. H. J. *Cell* **2005**, *123*, 1191–1198.
- (7) Tomasz, M.; Palom, Y. *Pharmacol. Ther.* **1997**, *76*, 73–87.
- (8) Smeaton, M. B.; Hlavin, E. M.; McGregor Mason, T.; Noronha, A. M.; Wilds, C. J.; Miller, P. S. *Biochemistry* **2008**, *47*, 9920–9930.
- (9) Puri, N.; Majumdar, A.; Cuenoud, B.; Miller, P. S.; Seidman, M. M. *Biochemistry* **2004**, *43*, 1343–1351.
- (10) Grant, K. B.; Dervan, P. B. *Biochemistry* **1996**, *35*, 12313–12319.

- (11) Weng, X.; Ren, L.; Weng, L.; Huang, J.; Zhu, S.; Zhou, X.; Weng, L. *Angew. Chem., Int. Ed.* **2007**, *46*, 8020–8023.
- (12) Halila, S.; Velasco, T.; De Clercq, P.; Madder, A. *Chem. Commun.* **2005**, 936–938.
- (13) Alzeer, J.; Schärer, O. D. *Nucleic Acids Res.* **2006**, *34*, 4458–4466.
- (14) Ali, M. M.; Nagatsugi, F.; Mori, K.; Nagasaki, Y.; Kataoka, K.; Sasaki, S. *Angew. Chem., Int. Ed.* **2006**, *45*, 3136–3140.
- (15) Hong, I. S.; Ding, H.; Greenberg, M. M. *J. Am. Chem. Soc.* **2006**, *128*, 485–491.
- (16) Hong, I. S.; Greenberg, M. M. *J. Am. Chem. Soc.* **2005**, *127*, 3692–3693.
- (17) Ding, H.; Greenberg, M. M. *Chem. Res. Toxicol.* **2007**, *20*, 1623–1628.
- (18) Hong, I. S.; Ding, H.; Greenberg, M. M. *J. Am. Chem. Soc.* **2006**, *128*, 2230–2231.
- (19) Hong, I. S.; Greenberg, M. M. *J. Am. Chem. Soc.* **2005**, *127*, 10510–10511.
- (20) Peng, X.; Greenberg, M. M. *Nucleic Acids Res.* **2008**, *36*, e31.

Scheme 1. Cross-Link Formation via Radical and Oxidative Mechanisms**Scheme 2.** Alternative Pathways for Cross-Link Formation

stringent washings and enables signal amplification that reduces the need for PCR amplification. Hydroxyl radical cleavage experiments revealed that the cross-links produced via the oxidative pathway also exclusively involve the opposing dA. Although stability studies suggested that the radical and oxidative pathways yield the same product **5**, direct evidence for this and the exact structure of the product(s) were lacking.^{15,18} We now describe one- and two-dimensional NMR experiments using doubly isotopically labeled (¹³C, ¹⁵N) oligonucleotides that provide definitive structural evidence for the cross-linked product. In addition, NMR and kinetic experiments provide mechanistic details that will be useful in future applications of the cross-linking chemistry attributable to **2** and related molecules.²¹

The monomeric components (**1** and dA) in the dimeric nucleoside **6** obtained following enzyme digestion of the ICLs formed under radical and oxidative conditions were bonded to one another via the C₅ methylene of the thymidine derived from **2** and the N₆ amino group of dA. It was inconceivable that such a connectivity in **6** could form directly via a radical reaction (Scheme 1).¹⁶ Inspection of molecular models suggested that N₁-dA is the most likely site of reaction with the radical when the nucleotide is in its syn conformation. Furthermore, consideration of nitrogen nucleophilicities also pointed to N₁ alkylation by the rearranged selenoxide **4** formed under oxidative conditions.^{22,23} We hypothesized that the radical and methide-type intermediates (**1** and **4**, respectively) reacted at N₁-dA to produce a kinetic product **5** that rearranged to **6** during the isolation procedures (Scheme 1). Reaction between the exocyclic

methylene carbon of the modified thymine and the opposing N₁-dA requires that the pyrimidine adopt the syn conformation. Previous kinetic competition studies suggested that rotation about the glycosidic bond was rate-limiting for cross-linking via the radical.¹⁵ For reaction via the longer-lived methide-type intermediate **4**, the rate constant for rotation about the glycosidic bond is less crucial. In addition, although we favored initial formation of **5**, reaction at C₆ of **1** and/or **4** followed by formal [3,3]-sigmatropic rearrangement of **7** could not be ruled out under either set of reaction conditions (Scheme 2). Finally, the potential cross-link products could be formed under oxidative conditions via S_N1, S_N2, and/or S_N2' mechanisms. The NMR and kinetic experiments described below address these questions.

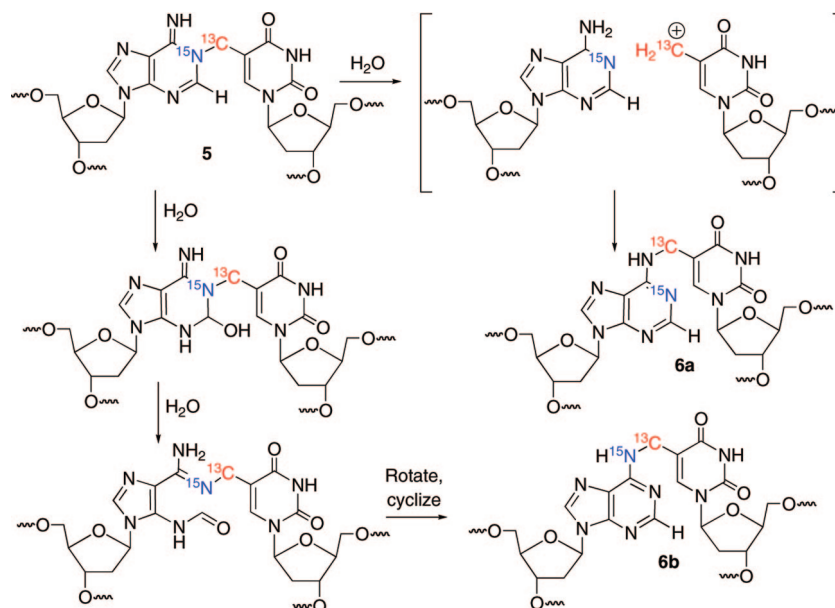
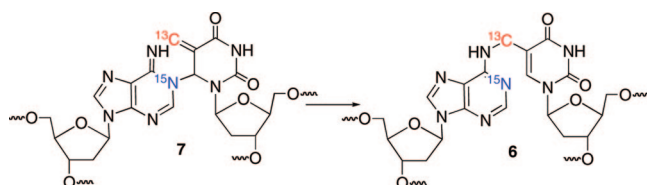
Results and Discussion

NMR Product Analysis and Mechanism of Isomerization Using Isotopically Labeled Oligonucleotides. We previously proposed that *syn*-**1** adds to N₁-dA to form **5** as a kinetic product that ultimately rearranges to the more stable N₆-alkylation product **6** (Scheme 1). Cross-link **5** was also proposed as the primary product when DNA containing **2** was exposed to oxidative conditions. Dissociative and associative rearrangement mechanisms are conceivable (Scheme 3), but kinetic experiments did not distinguish between them.¹⁵ These experiments also did not eliminate **7** as a possible product. NMR analysis of labeled oligonucleotides has proven useful in studies of cross-linked DNA.^{4,24} We recognized that carrying out the cross-linking

(21) Peng, X.; Hong, I. S.; Li, H.; Seidman, M. M.; Greenberg, M. M. *J. Am. Chem. Soc.* **2008**, *130*, 10299–10306.

(22) Weinert, E. E.; Frankenfield, K. N.; Rokita, S. E. *Chem. Res. Toxicol.* **2005**, *18*, 1364–1370.

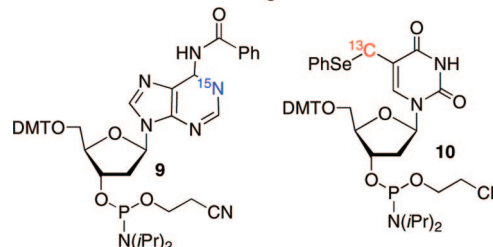
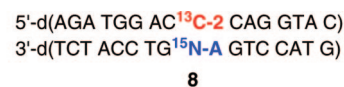
(23) Veldhuyzen, W. F.; Shallop, A. J.; Jones, R. A.; Rokita, S. E. *J. Am. Chem. Soc.* **2001**, *123*, 11126–11132.

Scheme 3. Structure and Mechanism Elucidation Using Isotopic Labeling**Scheme 4.** Mechanistic Distinction Using Double Isotopic Labeling

reaction using $^{13}\text{C}_5\text{-2}$ and $^{15}\text{N}_1\text{-dA}$ would enable direct detection of **5** and/or **7** (Schemes 3 and 4). In addition, the two possible rearrangement mechanisms involving **5** would also be distinguishable from one another using the doubly labeled duplex (Scheme 3). The N_1 -alkylation product **5** and subsequent formation of **6b** via an associative (Dimroth-like) rearrangement mechanism would be identifiable via J_{CN} and/or J_{HN} coupling in the products. In principle, coupling between $\text{H}_2\text{-dA}$ and $^{15}\text{N}_1\text{-dA}$ of the purine should be detected in **5**, but its presence in **6** depends upon the rearrangement mechanism. If the rearrangement proceeds via a dissociative mechanism to give **6a**, the coupling will be preserved, but it will be lost if an associative mechanism to give **6b** is involved (Scheme 3). The opposite is true for the J_{CN} coupling, as the connectivity between the labeled atoms in **5** is maintained during an associative rearrangement. The doubly labeled substrate also enables us to detect the third possible cross-linked product **7** and the rearrangement pathway that results from initial cross-linking between the C_6 position of the modified pyrimidine and $\text{N}_1\text{-dA}$ (Scheme 2). This pathway would be evident from an absence of significant J_{CN} coupling in the primary and rearrangement products (Scheme 4) as well as the distinctive chemical shift of the exocyclic methylene group.

These experiments were carried out on a duplex containing the same sequence as a 16 base pair substrate (**8**) previously shown to produce ICLs from **2** under radical and oxidative conditions and on the corresponding mononucleosides **11** and **12** (Scheme 5).^{15,16} The $^{15}\text{N}_1\text{-dA}$ phosphoramidite **9** was synthesized using procedures reported by Gao and Jones²⁵ and

Harris and co-workers²⁶ for synthesizing $^{15}\text{N}_1\text{-dA}$, which was converted to **9** via standard methods. Similarly, **10** was prepared via a slightly modified version of the route previously used to synthesize the unlabeled phosphoramidite.^{16,27} The ^{13}C label was



introduced via transmetalation of the bis(TBDPS) ether of 5-iodo-2'-deoxyuridine with $^{13}\text{CH}_3\text{I}$ using the procedure of Aso et al.²⁸ The oligonucleotide in **8** containing **2** was purified by reversed-phase HPLC following initial purification by denaturing polyacrylamide gel electrophoresis (PAGE) in order to remove any oligonucleotide containing 5-hydroxymethyl-2'-deoxyuridine, which is formed from adventitious oxidation of **2**. Gel electrophoresis was sufficient for purification of the oligonucleotide containing $^{15}\text{N}_1\text{-dA}$.

Initial NMR experiments were carried out using **11** and **12**, the labeled analogues of **2** and dA, respectively. Oxidation (NaIO_4 , 100 mM) of the nucleoside mixture (20 mM) in phosphate buffer (10 mM, pH 7.2) and NaCl (100 mM) followed by in situ analysis provided a spectrum consistent with **13** (**5**), as evidenced by a two-dimensional (2D) heteronuclear single-quantum correlation (HSQC) experiment that revealed correlation between the $\text{H}_2\text{-dA}$ proton (δ 8.65) and the ^{15}N -labeled N_1

(24) Young-Jin, C.; et al. *J. Am. Chem. Soc.* **2005**, *127*, 17686–17696.

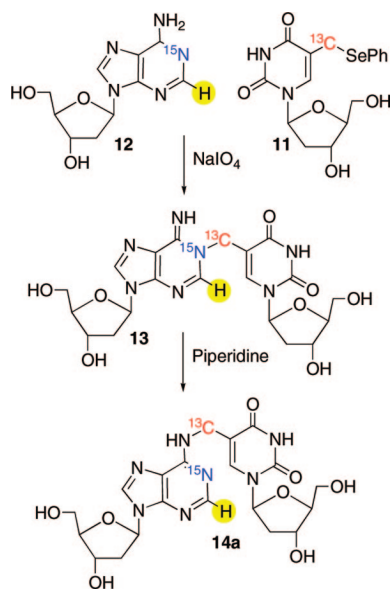
(25) Gao, X.; Jones, R. A. *J. Am. Chem. Soc.* **1987**, *109*, 1275–1278.

(26) Kim, H. H.; Finneman, J. I.; Harris, C. M.; Harris, T. M. *Chem. Res. Toxicol.* **2000**, *13*, 625–637.

(27) Hong, I. S.; Greenberg, M. M. *Org. Lett.* **2004**, *6*, 5011–5013.

(28) Aso, M.; Kaneko, T.; Nakamura, M.; Koga, N.; Suemune, H. *Chem. Commun.* **2003**, 1094–1095.

Scheme 5. Cross-Linking of Isotopically Labeled Monomers



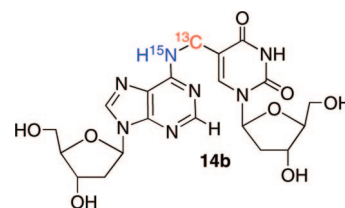
nitrogen derived from **11** (Figure 1A,B and Scheme 5). The ^{15}N carrier was positioned near 230 ppm, in the characteristic chemical shift range for aromatic ^{15}N resonances (200–230 ppm), and the HSQC pulse sequence parameters were adjusted to detect the long-range $\text{H}_2\text{--N}_1$ coupling constant (~ 15 Hz). To detect the J_{CN} coupling constant, two high-resolution, long-range $\text{H}_2\text{--N}_1$ HSQCs were acquired ($J_{\text{H}_2\text{N}_1} \approx 15$ Hz), one in the presence and the other in the absence of ^{13}C decoupling in the ^{15}N (ω_1) dimension. In the presence of ^{13}C decoupling (Figure 1A), the $\text{H}_2\text{--N}_1$ cross-peak appears as a singlet. In the absence of ^{13}C decoupling (Figure 1B), the $\text{H}_2\text{--N}_1$ cross-peak splits into a doublet due to the J_{CN} coupling constant. The small offset between the two components of the N–C doublet in the ^1H (ω_2) dimension is the consequence of a small, long-range $\text{H}_2\text{--}^{13}\text{C}$ coupling ($J_{\text{H}_2\text{C}}$). Since no ^{13}C decoupling is employed anywhere in the HSQC pulse sequence, the ^{13}C spin states ($\text{C}\uparrow$ and $\text{C}\downarrow$) are completely undisturbed throughout the experiment. This results in the observation of exclusive correlations between N_1 nitrogens and H_2 protons associated with $\text{C}\uparrow$ spins [$\text{N}_1(\text{C}\uparrow)$ (ω_1) \rightarrow $\text{H}_2(\text{C}\uparrow)$ (ω_2)] and N_1 nitrogens and H_2 protons associated with $\text{C}\downarrow$ spins [$\text{N}_1(\text{C}\downarrow)$ (ω_1) \rightarrow $\text{H}_2(\text{C}\downarrow)$ (ω_2)], also called an E.COSY^{29,30} effect. The displacement between the two peaks is equal to $J_{\text{H}_2\text{C}}$. Exposure of dimeric nucleoside **13** to piperidine to facilitate rearrangement to **14a** (**6a**) yielded the expected product, as evidenced by a comparison of the resulting ^1H NMR and HPLC data to those previously reported.¹⁶ A $\text{H}_2\text{--N}_1$ HSQC experiment revealed that the ^{15}N label was still adjacent to $\text{H}_2\text{--dA}$ in **14a** (Figure 1C), indicating that the rearrangement proceeded at least in part via a dissociative mechanism. However, we cannot rule out the possibility that a portion of the reaction proceeds via an associative mechanism for the following two reasons: (a) the NMR experiments were carried out in D_2O solvent, thus precluding the observation of labile H_6 protons on the exocyclic amine (N_6) in **14a**; (b) even in H_2O solvent, rapid exchange of the H_6 protons may prevent observation of $\text{H}_6\text{--N}_6$ cross-peaks in the HSQC experiment.

(29) Griesinger, C.; Sørensen, O. W.; Ernst, R. R. *J. Am. Chem. Soc.* **1985**, *107*, 6494–6496.

(30) Montelione, G. T.; Wagner, G. *J. Am. Chem. Soc.* **1989**, *111*, 5474–5475.

The experiment utilizing isotopically labeled monomeric components (Figure 1, Scheme 5) proved to be very useful for subsequent studies in duplex **8**. NMR was again used to characterize the crude mixture of products obtained from reaction of **8** (1.0 mM) with NaIO_4 (5 mM) in potassium phosphate (10 mM, pH 7.2) and NaCl (100 mM). Consistent with the experiment in which monomeric molecules were employed, a resonance was observed in the proton dimension at δ 7.90, which was correlated with the ^{15}N coupled to the ^{13}C (Figure 2A,B). Comparable results were obtained when **8** (1.5 mM) was photolyzed to produce **1**, although the signal-to-noise ratio was not as great because of a lower cross-link yield.³¹ Following consumption of **4** or photolysis of **2**, no signal consistent with that of **7** (Scheme 4) was detected, as evidenced by the absence of any ^1H signals in the δ 5.0–6.5 region, where the vinyl protons from the exocyclic methylene group were expected to resonate.^{19,21} These experiments provide definitive evidence for **5** as the primary cross-link product produced from phenyl selenide **2** under oxidative and radical conditions.

NMR also provided valuable mechanistic information regarding the rearrangement of **5** to **6** within duplex DNA. The crude cross-linked sample was subjected to the previously employed purification and isolation conditions¹⁶ that gave rise to **6** but not to piperidine, as was used above for the product obtained from reaction of the monomers. The resulting HSQC NMR spectra failed to show any $\text{H}_2\text{--N}_1$ correlations (data not shown). Since the experiments utilizing the monomeric material proved that such a coupling was detectable, the absence of any such coupling in the rearranged polymeric cross-link suggested that in the duplex, **5** isomerizes via an associative (Dimroth-type) mechanism to **6b** (Scheme 3).³² We also considered the possibility that the absence of coupling between the $^{15}\text{N}_6$ in **6b** and the adjacent protons or ^{13}C might be due to larger coupling in the monomeric material than in the duplex. Consequently, we digested the rearranged cross-link product and purified **14b**, the nucleoside form of **6b**. In D_2O solvent, the NMR spectra



again failed to show an $\text{H}_2\text{--N}_1$ correlation (data not shown). The absence of coupling between the exocyclic amine in **6b** and the adjacent magnetically active nuclei, which would appear as $\text{H}_6\text{--N}_6$ cross peaks, is attributed to rapid exchange of the labile H_6 protons with water, especially under non-hydrogen-bonded conditions. Splittings due to J_{CN} couplings (between the exocyclic adenine nitrogen and the exocyclic methylene carbon on the thymine) could not be observed in high-resolution $^1\text{H}\text{--}^{13}\text{C}$ HSQC spectra either, because the cross-peaks were too broad, indicating intermediate conformational-exchange broadening or conformational heterogeneity in the cross-link region. Subsequently, we attempted to detect the J_{CN} coupling via $^{15}\text{N}\text{--}^{13}\text{C}$ splittings in an $\text{H}_6\text{--N}_6$ HSQC correlation spectrum. Accordingly, the sample was lyophilized and redissolved in 95:5 $\text{H}_2\text{O}/\text{D}_2\text{O}$ acetate buffer (10 mM, pH 5.0). The HSQC parameters were adjusted to detect the $\text{H}_6\text{--N}_6$ correlation via the one-

(31) See the Supporting Information.

(32) Fujii, T.; Itaya, T. *Heterocycles* **1998**, *48*, 359–390.

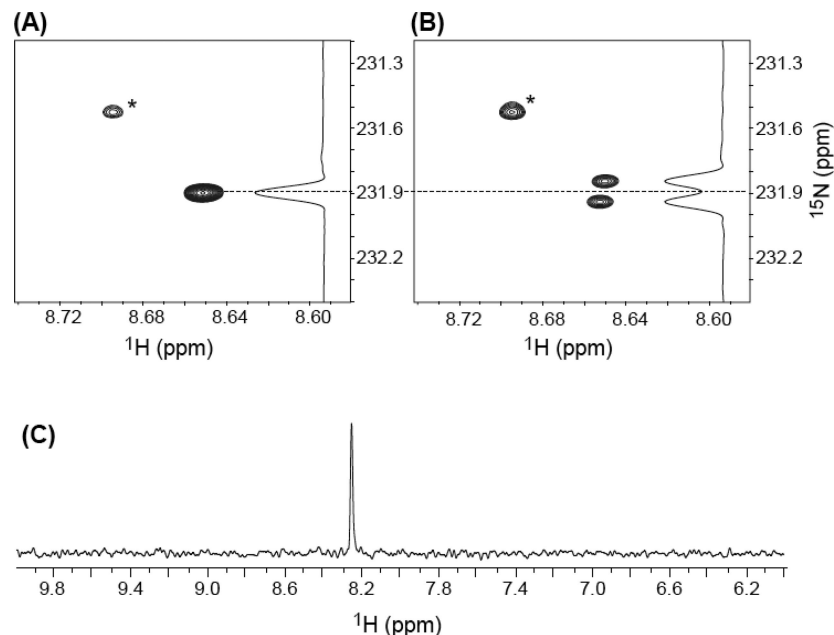


Figure 1. NMR analysis of the reaction of **11** ($^{13}\text{C}_5\text{-2}$) and **12** ($^{15}\text{N}_1\text{-dA}$) in the presence of NaIO_4 . (A, B): 2D $\text{H}_2\text{-N}_1$ HSQC of the crude reaction mixture acquired at high resolution (0.47 Hz/point) in the ^{15}N dimension in (A) the presence and (B) the absence of ^{13}C decoupling in the ^{15}N dimension. The peaks marked with * in (A) and (B) belong to unreacted starting material. The contour thresholds are not identical in (A) and (B). (C) 1D HSQC of HPLC-purified **14a** following rearrangement of **13** induced by piperidine.

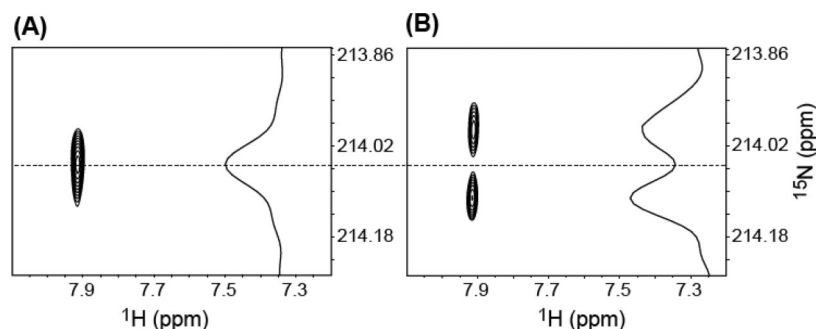


Figure 2. NMR analysis of the reaction of **8** in the presence of NaIO_4 . (A, B): 2D $\text{H}_2\text{-N}_1$ HSQC of the crude reaction mixture acquired at high resolution (0.47 Hz/point) in the ^{15}N dimension in (A) the presence and (B) the absence of ^{13}C decoupling in the ^{15}N dimension. Peaks belonging to unreacted starting material are not shown. The contour thresholds are not identical in (A) and (B).

bond $J_{\text{H}_6\text{N}_6}$ coupling (~ 90 Hz), and the ^{15}N carrier was positioned at 80 ppm, which is characteristic of the exocyclic N_6 resonance and very distinct from the aromatic N_1 resonance (200–230 ppm). A low-resolution HSQC (Figure 3) clearly shows the H_6 proton ($\delta \approx 7.55$ ppm) correlated with a ^{15}N resonance at 83.3 ppm. This unequivocally establishes that the ^{15}N label is at the exocyclic N_6 position (**14b**), which is positive evidence in support of the associative mechanism (Scheme 3). Attempts to detect a J_{CN} coupling by recording high-resolution spectra with and without ^{13}C decoupling were unsuccessful because the ^{15}N resonance was rather broad and decayed rapidly. This observation is consistent with the similar broadening observed in the ^{13}C resonances in the $^1\text{H}\text{-}^{13}\text{C}$ HSQC spectra, indicating mobility on an intermediate exchange time scale in the cross-linked region.

The change in mechanism for the rearrangement of **5** to **6b** in the duplex compared with that for the monomeric system (**13** to **14**) is ascribed to differences in reaction conditions. More pertinent is the question of why the associative rearrangement mechanism of **5** to **6b** in DNA is distinct from the behavior observed for the *o*-quinone methides studied by Rokita and co-workers,^{22,23,33,34} which react reversibly with DNA via a

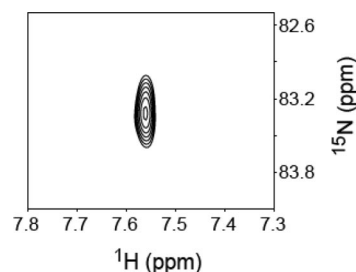


Figure 3. NMR analysis of **14b** obtained following enzyme digestion of the cross-linked product produced in the reaction of **8** with NaIO_4 . $^1\text{H}\text{-}^{15}\text{N}$ HSQC of the crude reaction mixture in 95:5 $\text{H}_2\text{O}/\text{D}_2\text{O}$ acetate buffer (10 mM, pH 5.0), acquired at low resolution in the ^{15}N dimension (20.0 Hz/point), showing a cross-peak between the exocyclic H_6 proton and N_6 nitrogen. The ^{15}N excitation frequency was positioned at 80 ppm, and the HSQC parameters were optimized to detect the one-bond J_{HN} coupling constant (90 Hz).

dissociative mechanism (Scheme 6). We speculate that the dissociative mechanism for **5** is less favorable than for the Rokita methides because the latter have a relatively acidic proton (the phenolic H) whose removal drives the reaction toward *o*-quinone

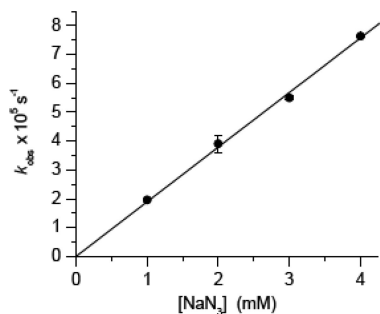
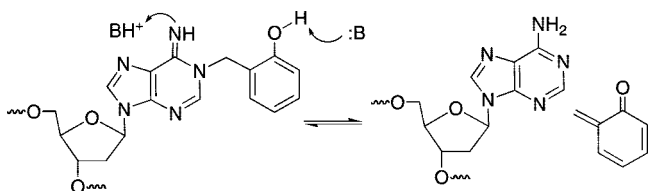


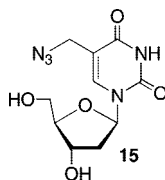
Figure 4. Observed rate constant for the formation of **15** upon reaction of azide with monomeric **4** as a function of azide concentration.

Scheme 6. Dissociative, Reversible Alkylation by an *o*-Quinone Methide



regeneration. A similar pathway is not available to the kinetic cross-link product **5** described in these studies.

Kinetic Determination of Cross-Link Formation Under Oxidative Conditions. Formation of **5** via the oxidative pathway that proceeds through **4** could occur via an S_N1 or S_N2' pathway. These were distinguished from one another by using UV absorption spectroscopy at 25 °C to measure the rate constant for the reaction of azide with monomeric **4** produced by oxidation of **11**. Absorption spectroscopy was a convenient tool for following this reaction because the methide **4** absorbs weakly in the 260–270 nm region where the maxima for nucleosides are typically observed. Hence, the absorption increase at 270 nm was used to measure formation of the product **15**. Azide



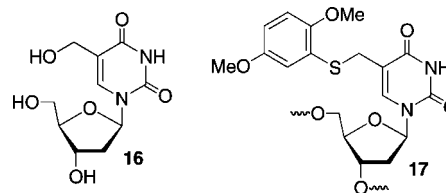
was used as a nucleophile instead of dA in order to avoid interference with the absorption spectrum of the product. This was particularly important since the nucleophile was present in large excess in order to fulfill the requirements of pseudo-first-order reaction conditions. The observed rate constant for the reaction of azide with monomeric **4** to produce **15** exhibited a linear dependence on nucleophile concentration (Figure 4) and is consistent with the S_N2' mechanism. These data yield a bimolecular rate constant of $1.9 \times 10^{-2} \text{ M}^{-1} \text{ s}^{-1}$ for the reaction of monomeric **4** with azide. Extrapolation to the reaction between the **4** and dA in a duplex suggests that cross-link formation under oxidative conditions also occurs via an S_N2' pathway. Attack by the nucleophile on the carbon of the allylic phenyl selenate **4** is atypical for this molecular family.^{35–38} However, the more typical attack on selenium to produce the

allylic alcohol is probably less favorable in this case because it would produce the unstable (nonaromatic) product, whereas reaction at the exocyclic methylene in **4** regenerates the aromatic pyrimidine ring.

Rate-Limiting Glycosidic Bond Rotation in Radical-Mediated Cross-Link Formation. Formation of **5** requires that the methide **4** or radical **1** adopt the syn conformation by rotating about the glycosidic bond. DNA breathing limits the rate at which rotation occurs. Although the rate constants for base-pair opening in duplexes containing **2** (or **4**) have not been measured, NMR studies on other duplexes suggest that rate constants $\geq 10^3 \text{ s}^{-1}$ at 25 °C are possible.^{39–41} This time scale is short compared with that on which the methide reacts to form cross-links but not that for a radical, whose lifetime is inherently more limited.¹⁸ The rate constant for ICL formation (k_{ICL}) from **1** was estimated by carrying out competition studies with thiol (RSH) under anaerobic conditions (eq 1):

$$\frac{[\text{ssDNA}]}{[\text{ICL}]} = \frac{k_{\text{RSH}}}{k_{\text{ICL}}} [\text{RSH}] + \frac{k_{\text{X}}}{k_{\text{ICL}}} \quad (1)$$

where k_{RSH} is the rate constant for the reaction involving the thiol. When the radical was flanked on both sides by dC, phenyl selenide **2** and aryl sulfide **17** were employed separately as photochemical precursors. In addition, glutathione (GSH) and β -mercaptoethanol (BME) were used as thiols. The magnitudes of the rate constants were affected by the presence of 5-hydroxymethyl-2'-deoxyuridine (**16**) and background levels of ICLs. Hence, it was imperative that HPLC-purified oligonucle-



otides from which oligonucleotides containing **16** had been removed as well as freshly hybridized duplexes be used for these experiments. Failure to remove the impurities gave rise to artificially high calculated values for k_{ICL} . The rate constants for ICL formation determined using **17** and **2** were indistinguishable from each other (Table 1) and were a factor of ~ 4 smaller than that reported previously using oligonucleotides that were not HPLC-purified.¹⁵ Furthermore, if one assumes that BME and GSH react with 5-(2'-deoxyuridinyl)methyl radical **1** with equal rate constants, one obtains k_{ICL} values that are within experimental error of one another.⁴²

Altering the flanking sequence has a more significant effect on ICL yields, as measured by phosphorimage analysis of ³²P-labeled substrates separated by denaturing PAGE. The cross-link yields in the absence of thiol (Table 1) were greater when 5-(2'-deoxyuridinyl)methyl radical **1** was flanked by pyrimidines than by purines. We attribute this to more efficient intrastrand

- (33) Wang, H.; Wahi, M. S.; Rokita, S. E. *Angew. Chem., Int. Ed.* **2008**, *47*, 1291–1293.
 (34) Zhou, Q.; Rokita, S. E. *Proc. Nat. Acad. Sci. U.S.A.* **2003**, *100*, 15452–15457.

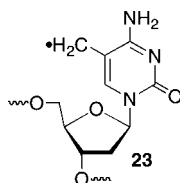
- (35) Reich, H. J.; Yelm, K. E.; Wollowitz, S. *J. Am. Chem. Soc.* **1983**, *105*, 2503–2504.
 (36) Bourland, T. C.; Carter, R. G.; Yokochi, A. F. T. *Org. Biomol. Chem.* **2004**, *2*, 1315–1329.
 (37) Nishibayashi, Y.; Uemura, S. *Top. Curr. Chem.* **2000**, *208*, 201–233.
 (38) Johnston, M.; Raines, R.; Walsh, C.; Firestone, R. A. *J. Am. Chem. Soc.* **1980**, *102*, 4241–4250.
 (39) Parker, J. B.; Bianchet, M. A.; Krosky, D. J.; Friedman, J. I.; Amzel, L. M.; Stivers, J. T. *Nature* **2007**, *449*, 433–437.
 (40) Snoussi, K.; Leroy, J. L. *Biochemistry* **2002**, *41*, 12467–12474.
 (41) Guéron, M.; Leroy, J. *Methods Enzymol.* **1995**, *261*, 383–413.
 (42) Newcomb, M. *Tetrahedron* **1993**, *49*, 1151–1176.

Table 1. Effect of the Flanking Sequence on ICL Formation from 5-(2'-Deoxyuridinyl)methyl Radical **1**

	$k_{\text{ICL}} \times 10^{-3} (\text{s}^{-1})^{\text{a}}$		Max. ICL Yd. (%) ^b
	BME	GSH	
5'-d(AGA TGG AC17 CAG GTA C) 3'-d(TCT ACC TG A GTC CAT G) 18	5.4 ± 0.7	5.4 ± 1.3	17.0 ± 0.4
5'-d(AGA TGG AC2 CAG GTA C) 3'-d(TCT ACC TGA GTC CAT G) 19	4.7 ± 0.7	5.8 ± 1.0	15.7 ± 0.2
5'-d(AGA TGG AG2 GAG GTA C) 3'-d(TCT ACC TCA CTC CAT G) 20	1.5 ± 0.1	n.d.	11.3 ± 1.0
5'-d(AGA TGG AT2 TAG GTA C) 3'-d(TCT ACC TAA ATC CAT G) 21	1.2 ± 0.1	n.d.	17.5 ± 2.4
5'-d(AGA TGG AA2 AAG GTA C) 3'-d(TCT ACC TTA TTC CAT G) 22	n.d.	n.d.	5.6 ± 1.0

^a Each rate constant is the average of at least two experiments, each carried out in triplicate. ^b For the reaction carried out in the absence of thiol. Each value is the average of at least three measurements.

cross-link formation when **1** is flanked by purines. Addition of **1** (and the analogous radical **23** generated from 5-methyl-2'-deoxycytidine) to the C₈ position of dG has been well-studied, and the subsequently formed tandem lesions are biologically significant.^{43–45} In contrast, tandem lesions resulting from



addition of **1** or **23** to an adjacent pyrimidine have been observed less frequently and are not as well studied.^{46,47} Although it is unknown if this is due to a smaller rate constant for addition by the radicals to pyrimidines than to purines, such a scenario is consistent with the phenomenological observations reported in the literature. The maximum ICL yields and cross-linking

rate constants were uncorrelated. ICL formation was the fastest when the **1** was flanked by dC, and it was not possible to accurately measure k_{ICL} when dA was the flanking nucleotide because the yield was already too low in the absence of thiol to accurately measure the change in the product as a function of thiol concentration. The reactivity of 5-(2'-deoxyuridinyl)methyl radical **1** was in contrast to that of **4**, whose rate constants for ICL formation were greater when flanked by pyrimidines but produced comparable yields of cross-links in all sequences.²⁰ Regardless, the most significant observation is that k_{ICL} is within the range that one would expect for the rate constant for nucleotide flipping and consistent with the previous proposal that isomerization of the radical into the syn conformation is the rate-determining step in ICL formation from **1**.^{15,39–41}

Conclusions

NMR analyses of synthetic oligonucleotides containing ¹³C and ¹⁵N labels have provided definitive proof for the kinetic product **5** formed by a novel DNA radical cross-linking reaction. The NMR experiments also prove that the same product is obtained via an oxidative pathway and that the initially formed product isomerizes to the thermodynamic cross-link **6b** via an associative mechanism in duplex DNA. The mechanism of the rearrangement is distinct from that involving *o*-quinone methides and suggests that the cross-links produced via **2** are chemically robust.³⁴ The irreversible nature of this cross-linking reaction suggests that it will be useful for kinetically trapping molecules in its vicinity. In this regard, kinetic experiments suggest that radical reactions will be influenced by the rate constant for isomerization about the glycosidic bond and that the reactivity of the methide-like species **4** is controlled by the rearomatization driving force. Knowledge of the mechanistic aspects of this chemistry will be useful in developing applications of the phenyl selenide precursor **2** as well as in the design of molecules with similar reactivity.^{20,21}

Acknowledgment. We are grateful for support of this research by the National Institute of General Medical Sciences (GM-054996 to M.M.G. and GM-075310 to J.R.T.) and the NSF (MCB-0615786 to J.R.T.). M.M.G. thanks Professor Ned Porter for a helpful discussion that provided the impetus for the NMR experiments.

Supporting Information Available: Complete description of experimental procedures, NMR spectra of **9** and **10**, HSQC spectra of the cross-link product formed from photolysis of **8**, and complete ref 24. This material is available free of charge via the Internet at <http://pubs.acs.org>.

JA807845N

- (43) Romieu, A.; Bellon, S.; Gasparutto, D.; Cadet, J. *Org. Lett.* **2000**, *2*, 1085–1088.
 (44) Zhang, Q.; Wang, Y. *Nucleic Acids Res.* **2005**, *33*, 1593–1603.
 (45) Jiang, Y.; Hong, H.; Cao, H.; Wang, Y. *Biochemistry* **2007**, *46*, 12757–12763.
 (46) Friedel, M. G.; Pieck, J. C.; Klages, J.; Dauth, C.; Kessler, H.; Carell, T. *Chem.—Eur. J.* **2006**, *12*, 6081–6094.
 (47) Cheek, J.; Broderick, J. B. *J. Am. Chem. Soc.* **2002**, *124*, 2860–2861.